and Ehrlich carcinoma. The cross-reactivity with murine livers and tumors may be due to the similar structure of rabbit and mouse enzymes. The failure of reactivity of the enzyme from MH 134 and Ehrlich carcinoma may be due to the existence of BLMase isozyme or contamination by related proteins.

Umezawa et al. (1974) purified BLMase from mouse liver by affinity chromatography using Sepharose 4B–lysinamide and obtained 25-fold-purified enzyme. However, further purification failed, because of the lability of the enzyme. In this respect the immunoaffinity with monoclonal antibody is extremely effective because rapid purification is expected. The two-step rapid purification procedure with immunoaffinity and subsequent DEAE-Toyopearl chromatography enabled us to obtain pure enzyme, which gives a single band in SDS–PAGE. We had first tried to bind anti-BLMase IgM directly to cyanogen bromide activated Sepharose. However, the coupled antibody showed reduced reactivity with the enzyme. Therefore, anti-BLMase monoclonal antibody was adsorbed on protein A–Sepharose coated with anti-mouse IgM.

The purified BLMase is inhibited by E-64, leupeptin, TLCK, and NEM but is enhanced by dithiothreitol. The results suggest that BLMase is a thiol enzyme. Comparison of the results with SDS–PAGE and those with HPLC gel filtration suggests that BLMase is a hexameric enzyme. Since purified BLMase is labile, partially purified enzyme was used for chromatofocusing. The pH of the active fraction eluted from the chromatofocusing column is in accordance with that of a single band shown by isoelectric focusing. The properties of BLMase indicate that BLMase is a previously unrecognized enzyme. The existence of BLMase in various tissues suggests that this enzyme could have a important physiological function.

References

Akiyama, S., Ikezaki, K., Kuramochi, H., Takahashi, K., & Kuwano, M. (1981) *Biochem. Biophys. Res. Commun. 101*, 55–60.

Bradford, M. M. (1976) *Anal. Biochem. 72*, 248–254.

Fahey, J. L., & Mckelvey, E. M. (1965) *J. Immunol. 94*, 84–90.

Galfre, G., & Milstein, C. (1981) *Methods Enzymol. 73*, 1–46.

Laemlli, U. K. (1970) *Nature (London) 227*, 680–685.

Lazo, J. S., Boland, C. J., & Schwartz, P. E. (1982) *Cancer Res. 42*, 4026–4031.

Matsukage, A., Yamaguchi, M., Tanabe, K., Nishizawa, M., Takahashi, T., Seto, M., & Takahashi, T. (1982) *Gann 73*, 850–853.

Miyaki, M., Ono, T., Hori, S., & Umezawa, H. (1975) *Cancer Res. 35*, 2015–2019.

Oakley, B. R., Kirsch, D. R., & Morris, N. R. (1980) *Anal. Biochem. 105*, 361–363.

Ozawa, S., Tamura, A., Suzuki, H., Nishimura, T., & Tanaka, N. (1985) *J. Antibiot. 38*, 1257–1265.

Sugimoto, Y., Suzuki, H., & Tanaka, N. (1983) *Biochem. Biophys. Res. Commun. 114*, 969–975.

Tanaka, S., Hu, S.-Z., Wang, T. S.-F., & Korn, D. (1982) *J. Biol. Chem. 257*, 8386–8390.

Umezawa, H., Takeuchi, T., Hori, S., Sawa, T., Ishizuka, M., Ichikawa, T., & Komai, T. (1972) *J. Antibiot. 25*, 409–420.

Umezawa, H., Hori, S., Sawa, T., Yoshioka, T., & Takeuchi, T. (1974) *J. Antibiot. 27*, 419–424.

500-MHz Proton Homonuclear Overhauser Evidence for Additional Base Pairs in the Common Arm of Eukaryotic Ribosomal 5S RNA: Wheat Germ†

Shi-Jiang Li,‡,§ Jiejun Wu,‡ and Alan G. Marshall*,‡,∥

Departments of Biochemistry and Chemistry, The Ohio State University, Columbus, Ohio 43210

Received July 30, 1986; Revised Manuscript Received November 21, 1986

ABSTRACT: A "common-arm" fragment from wheat germ (*Triticum aestivum*) 5S RNA has been produced by enzymatic cleavage with RNase T1 and sequenced via autoradiography of electrophoresis gels for the end-labeled fragments obtained by further RNase T1 partial digestion. The existence, base pair composition, and base pair sequence of the common arm are demonstrated for the first time by means of proton 500-MHz nuclear magnetic resonance. From Mg^{2+} titration, temperature variation, ring current calculations, sequence comparisons, and proton homonuclear Overhauser enhancement experiments, additional base pairs in the common arm of the eukaryotic 5S RNA secondary structure are detected. Two base pairs, G_{41}·C_{34} and A_{42}·U_{33} in the hairpin loop, could account for the lack of binding between the conserved GAAC segment of 5S RNA and the conserved Watson–Crick-complementary GTΨC segment of tRNAs.

5S RNA is an essential structural component in all ribosomes and is necessary for protein synthesis (Pieler et al., 1984). It is widely believed that at least the eukaryotic 5S RNAs share a common secondary structure [e.g., see Delihas et al. (1984)]. Three universal base-pairing schemes have been adapted to the primary sequence of wheat germ 5S RNA in Figure 1. In particular, each model contains a "common arm" extending from bases corresponding to residues 26–56 in the wheat germ primary sequence. A similar arm is proposed for eukaryotic 5.8S RNA (Lee & Marshall, 1986).

Many early models for 5S RNA did not contain the common-arm helical segment (Boedtker & Kelling, 1967; Brownlee et al., 1972; Du Buy & Weissman, 1971; Monier, 1974). However, once a three-stem model based upon comparative sequence analysis was proposed (Fox & Woese, 1975), all subsequently proposed 5S RNA secondary structures shared a common-arm segment (Delihas et al., 1984; Luoma & Marshall, 1978a,b; Osterberg et al., 1976; Studnicka et al., 1981; de Wachter et al., 1982; Luehrsen & Fox, 1981).

† This work was supported by grants (to A.G.M.) from the U.S. Public Health Service (NIH 1 R01 GM-29274 and NIH 1 S10 RR-01458) and The Ohio State University.

‡ Department of Biochemistry.

§ Present address: NMR Research, Johns Hopkins Medical Institute, Baltimore, MD 21205.

∥ Department of Chemistry.

0006-2960/87/0426-1578$01.50/0

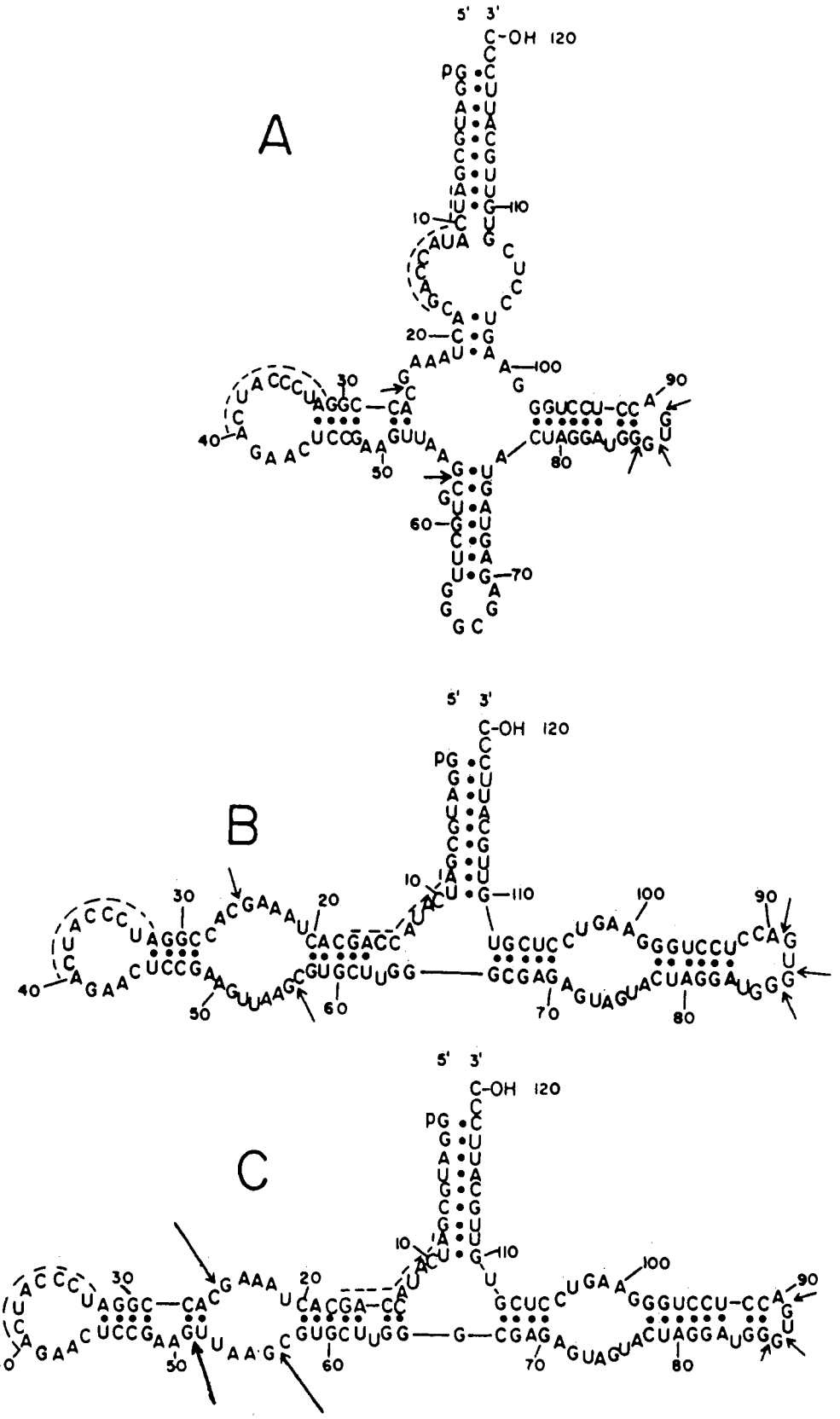

FIGURE 1: Proposed secondary base-pairing schemes for 5S RNA, adapted to the primary nucleotide sequence of wheat germ 5S RNA. (A) Cloverleaf model (Luoma & Marshall, 1978a,b). (B) Three-stem model (Luehrsen & Fox, 1981). (C) Modified Fox–Woese model (Studnicka et al., 1981). The common-arm fragment is the segment extending from C_{26} to G_{51}, and the core fragment is what remains after removal of residues 26–56 (see large arrows in Figure 1C).

Unfortunately, the common-arm structure presents an immediate puzzle regarding 5S RNA function. The unpaired segment GAAC is conserved for most 5S RNA primary sequences and is Watson–Crick complementary to the similarly conserved GTΨC segment of tRNAs. Therefore, it seemed logical to infer that these two segments might pair together to help anchor tRNA to the 5S RNA site on the large ribosomal subunit during protein synthesis (Brownlee et al., 1968), particularly since protein synthesis was inhibited by addition of free GTΨC oligonucleotide to ribosomes (Ofengand &

Henes, 1969). However, direct pairing between GAAC of free *Escherichia coli* 5S RNA and GTΨC in solution could not be demonstrated (Erdmann et al., 1973). Moreover, excision of the GAAC segment, followed by reconstitution of the excised 5S RNA into ribosomes, gave a functional ribosome (Pace et al., 1982; Zagorska et al., 1984; Noller, 1984). Attempts to account for these observations have included a proposed "dynamic" structure for the common arm (Vandenberge et al., 1984) and participation of the common arm in a transition between "A" and "B" forms (Pieler et al., 1984). Alternatively, lack of enzymatic cleavage has been interpreted to imply tertiary base pairing in the common-arm region (Pieler & Erdmann, 1982).

The most direct and definitive technique for identification, assignment, and sequencing of RNA base pairs is proton homonuclear Overhauser enhancement (NOE) experiments (Johnston & Redfield, 1978). Although the common arm appears in virtually all proposed secondary structures for 5S RNA, the base pairs from that arm have not yet been assigned by direct proton NMR observations, primarily because the large number of overlapping resonances in the base pair hydrogen-bond region (10–15 ppm) of the spectrum has effectively prevented the unambiguous assignment of NOE connectivity (and thus base pair sequence) for that 5S RNA segment.

In the present paper, we use RNase T1 enzymatic cleavage of wheat germ 5S RNA to generate common-arm and core fragments, whose 500-MHz proton NMR spectra are much simpler than that of intact wheat germ 5S RNA. Mg^{2+} titration, temperature dependence, ring current calculations, and ^1H NOE experiments performed on the fragments then provide direct evidence for the existence and base pair composition of the common-arm fragment. The previously proposed minimal four-pair common-arm helical segment (Fox & Woese, 1975) is found to be insufficient to account for the observed base pair number and spatial connectivity, and a revised common-arm model containing additional base pairs (de Wachter et al., 1982) is supported by the present results.

Materials and Methods

Wheat Germ 5S RNA. Wheat germ (*Triticum aestivum*) was a gift from International Multifoods (Columbus, OH). 5S RNA was isolated by sodium dodecyl sulfate (SDS)/phenol extraction, followed by DE-32 ion-exchange chromatography and Sephadex G-75 gel filtration as described by Li et al. (1984).

Production and Isolation of RNase T1 Cleavage Fragments of Wheat Germ 5S RNA. We have previously reported a procedure for isolating the 5S RNA fragment formed by RNase T1 primary cleavage at residues 86, 87, and/or 89 (Li & Marshall, 1986). In this paper, we report conditions for producing fragments formed by additional secondary cleavage at residues 25 and 51. Ethanol-precipitated purified wheat germ 5S RNA was dissolved in 0.3 M NaCl/10 mM tris(hydroxymethyl)aminomethane (Tris) base, pH 7.5, to give a final RNA concentration of 1 mg/mL. 1000 units of RNase T1 (Boehringer-Mannheim, 100 units/μL) was added per milligram of RNA to initiate enzymatic cleavage. After 20 min at room temperature, the enzyme was inactivated by addition of an equal volume of 5% SDS and phenol. The reaction mixture was then centrifuged at 10000*g* for 5 min. RNA was recovered from the aqueous supernate by precipitation with 2.5 volumes of cold (−20 °C) ethanol.

The RNase T1 digestion products were then characterized by small-scale polyacrylamide gel electrophoresis (PAGE) under nondenaturing conditions. The gel consisted of 10% acrylamide/bis(acrylamide) (19:1 w/w), 0.5% (w/v) ammonium persulfate, and 0.08% (v/v) *N,N,N′,N′*-tetramethylethylenediamine (TEMED). The electrophoresis buffer was 0.1 M KCl, 5 mM $MgCl_2$, and 50 mM Tris–borate, pH 7.8. Gels were run at 3 V/cm for 16 h at room temperature, and RNA was visualized by staining with methylene blue. The result of the gel scan is shown in Figure 2B. Another PAGE experiment under denaturing conditions (Li & Marshall, 1985b; at 12% rather than 8% gel concentration) was performed to assay the purity of the B_2 fragment from Sephadex G-75 chromatography (see below). The relative amount of RNA in each band on a gel was calculated from the relative peak area in an optical scan (550 nm) of the stained gel.

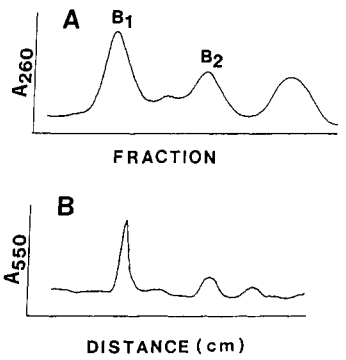

FIGURE 2: Nondenaturing gel filtration and electrophoresis patterns for the combined fragments from RNase T1 cleavage of wheat germ 5S RNA. (A) Sephadex G-75 nondenaturing gel permeation chromatography elution profile (2.5 × 150 cm column, 14 mL/h elution rate, collected as 7 mL/tube fractions. (B) Nondenaturing electrophoresis gel scan of the same sample. In both cases, the core (B_1) and common-arm (B_2) fragments are clearly resolved, confirming that gel filtration provides a good method for separation and purification of these two major RNA fragments.

Preparative-scale separation and isolation of fragments B_1 and B_2 were achieved via nondenaturing Sephadex G-75 gel filtration chromatography (150 × 2.5 cm column) with elution buffer of 1.0 M NaCl/10 mM Tris- base, pH 7.0. Of the three RNA peaks eluted from the Sephadex G-75 column (see Figure 2A), the third (i.e., the last) appeared to consist of small fragments (see Results and Discussion) and was discarded. The first two fractions, labeled B_1 and B_2 in Figure 2A, were separated and subjected to RNase T1 mapping. The procedure (BRL RNA Sequencing System; Bethesda Research Laboratories) consisted of initial 3′-dephosphorylation with calf alkaline phosphatase followed by 3′-end labeling with [5′-^{32}P]pCp via T4 RNA ligase, purification of the end-labeled fragments, RNase T1 partial digestion, and autoradiography of a subsequent sequencing electrophoresis gel. RNA sequencing was performed under the generous guidance of E. S. Maxwell in his laboratory at North Carolina State University.

NMR Samples. Preparation, determination of RNA concentration, and Mg^{2+} titration of NMR samples of intact wheat germ 5S RNA were as previously described (Li & Marshall, 1986). Wheat germ 5S RNA was dissolved in a solution containing 10 mM cacodylate in 95%/5% H_2O/D_2O, 100 mM NaCl, and 1 mM ethylenediaminetetraacetic acid (EDTA), pH 7.0, to give an RNA concentration of 30 mg/mL.

The RNase T1 cleavage fraction B_1 was dissolved in a buffer containing 10 mM EDTA and 10 mM sodium cacodylate at pH 7.0 and then dialyzed against the same buffer at a volume ratio of 1:500 for 4 h. The sample was further dialyzed against deionized water at a volume ratio of 1:1000 for 3 h and lyophilized. The lyophilized powder was dissolved in the same buffer as that for the intact 5S RNA sample. The core

fragment (B_1) concentration in the final NMR sample was 450 OD (A_{260}) units in 0.4 mL. A sample of the common-arm (B_2) fraction was prepared similarly, at a final concentration of 105 OD (A_{260}) units in 0.4 mL.

NMR Spectroscopy. Proton NMR spectra were obtained with a Bruker AM-500 spectrometer at 11.75 T (500 MHz for ^1H). Use of a 1331 hard-pulse sequence (Hore, 1983) (with in-line 20-dB attenuator) combined with alternate delayed acquisition (ADA) (Roth et al., 1980) resulted in water suppression by a factor of ca. 50000, with an essentially flat base line. 4K time-domain data sets were acquired at 296 K in about 0.173 s, with a total acquisition cycle time of 0.6 s which had been optimized according to T_1 relaxation time measurements (not shown). Proton homonuclear Overhauser enhancement (NOE) experiments were performed via 0.3-s preirradiation (0.2-mW decoupler power) of the resonance of interest, with a Redfield 21412 soft-pulse excitation (Redfield et al., 1975). Each displayed NOE (difference) spectrum was based on time-domain subtraction of 8000 on- from 8000 off-resonance (at 15.0 ppm) scans (Chang & Marshall, 1986), for a total acquisition time of about 4 h for each NOE difference spectrum.

Results and Discussion

RNase T1 Cleavage Sites for Wheat Germ 5S RNA. Although RNase T1 cleaves RNA at the 3′ side of guanosine (G) residues in single-stranded segments, not all G sites are cleaved at the same rate. For example, G residues participating in secondary or tertiary base pairing may not be accessible to enzymatic attack until the RNA structure has been partially unraveled by prior cleavage at other sites. Initial RNase T1 cleavage sites for rye 5S RNA reportedly occur at G residues 85, 86, and/or 88, with secondary cleavages at G residues 25 and 55; the fragment extending from base 25 to base 54 could then be separated from the rest of the rye 5S RNA via nondenaturing PAGE (Barber & Nichols, 1978; Payne & Dyer, 1976). A subsequently corrected nucleotide sequence of rye (Vandenberghe et al., 1984) now makes it identical with that of wheat germ (Mackay et al., 1980); therefore, we expect to observe RNase T1 cleavage at the same G residues for wheat germ 5S RNA. From the results of systematic variation in enzyme concentration, 5S RNA concentration, buffer composition, temperature, and reaction time, one can devise reaction conditions under which cleavage can be controlled to occur primarily at selected sites. Complete digestion at first- and second-order sites is essential for subsequent isolation of the desired fragments at high yield, as we showed in prior isolation and structural analysis of a wheat germ 5S RNA fragment containing the "tuned helix" (Li & Marshall, 1986).

Nondenaturing Sephadex G-75 chromatography and nondenaturing PAGE of RNase T1 cleaved wheat germ 5S RNA each reveal three well-resolved fractions (Figure 2). Because bases 1–25, 57–86 (and/or 87 and 89), and 90–120 are held together by base pair hydrogen bonds under nondenaturing conditions, their fragment (B_1) elutes first (Figure 2A) and is designated as the molecular core fragment. (In contrast to other eukaryotic 5S RNAs, wheat germ 5S RNA is not cleaved at G_{41} by RNase T1.) RNase T1 mapping confirmed that peak B_1 consists of segments containing at least residues 1–25 and 90–120. We presume that fraction B_1 also contains the segment from residues 57–86,87,88, which could not be resolved (via denaturing PAGE of fraction B_1) from residues 90–120 due to their similar size and PAGE mobility. In support of this interpretation, (a) the size of fragment B_1 can be estimated as about 90 bases from its Sephadex G-75 and PAGE mobilities, and (b) the segment from residues 57–88 was not detected in either of the other two G-75 peaks (see below). Thus, fraction B_1 appears to consist of three segments (residues 1–25, 57–86,87,88, and 90–120) held together under nondenaturing conditions by hydrogen bonds.

RNase T1 mapping showed that fraction B_2 in Figure 2 consisted mainly of residues 26–51, a minor component of residues 26–56, and some other contaminant fragments (residues 1–25, 2–25, and 7–25) adding up to about 20% of the total RNA based upon an optical scan of a denaturing (8 M urea) PAGE gel. The presence of minor fragments from the segment spanning residues 1–25 is somewhat surprising under nondenaturing conditions, since the molecular "stalk" or "stem" (see Figure 1) has been observed directly by proton NMR in 5S RNA from *Bacillus subtilis* (Chang & Marshall, 1986) and yeast (Chen & Marshall, 1986; Lee & Marshall, 1987). However, one should keep in mind that initial cleavage at one or more sites (as in this case) may act to destabilize and unfold other normally base-paired segments, making them accessible to further enzymatic cleavage.

In any case, the above-mentioned contaminants should not contribute to the downfield (9–15 ppm) proton NMR spectrum of the B_2 fraction, because (a) bases 1–25 cannot form a thermodynamically stable arrangement of Watson–Crick base pairs, according to a computer-based search (E. S. Maxwell, private communication), and (b) we find no evidence of pairing between residues 1–25 and 26–51,56 from either nondenaturing PAGE or Sephadex G-75 separations. Therefore, we henceforth denote fraction B_2 as the common-arm segment, not because it is chemically pure but because only that component of the fraction will contribute to the proton NMR spectral region of interest.

The third (unlabeled) peak from the nondenaturing Sephadex G-75 elution profile (Figure 2) evidently consists of very small RNA fragments which are not seen in denaturing PAGE experiments and which do not produce any signals in the 9–15 ppm region of a proton NMR spectrum. These fragments presumably include secondary digestion fragments (e.g., residues 52–56, possibly from cleavage of residues 26–56). Finally, the close similarity between the nondenaturing electrophoresis pattern (Figure 2B) and the nondenaturing gel filtration elution profile (Figure 2A) confirms that gel filtration provides a reliable means for isolating pure complementary core (B_1) and common-arm (B_2) fragments.

Structurally Complementary Common-Arm and Core Fragments Have Complementary ^1H NMR Spectra. RNase T1 mapping (see above) showed that the NMR-visible core and common-arm components of fractions B_1 and B_2 form essentially complementary (except for residues 52–56) structural segments. 500-MHz proton NMR spectra of intact wheat germ 5S RNA and its two major RNase T1 cleavage fragments are shown in Figure 3. The peak widths are narrower for the smaller core fragment (ca. 40 Hz) and common-arm fragment (ca. 20 Hz) than for the larger intact 5S RNA (ca. 55 Hz). As expected, the line widths for the core fragment resonances are quite similar to those for typical tRNAs (which have about the same molecular weight).

More detailed scrutiny reveals that virtually all of the base pair proton resonances seen in the intact 5S RNA can be located in one or the other of the two fragments. For example, the A·U's labeled "B" and "C" are located in the core fragment, whereas the A·U peaks labeled "A" are found in the common-arm fragment. In other words, the sum of the spectra of the two fragments is essentially the same as that of the intact 5S RNA. Since base pair hydrogen-bond proton resonance

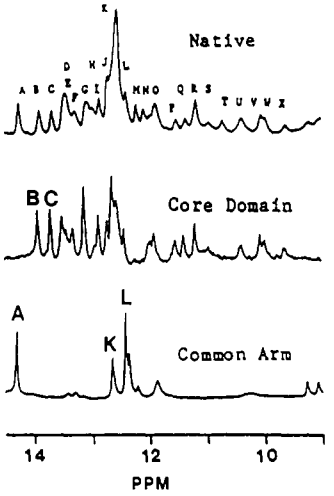

FIGURE 3: Proton 500-MHz ^{1}H NMR spectra corresponding to the secondary structures (see Figure 1) of intact wheat germ 5S RNA (top), the core fragment (middle), and the common-arm fragment (bottom). All samples are buffered in 95%/5% H_2O/D_2O containing 10 mM sodium cacodylate (pH 7.0), 100 mM NaCl, and 1 mM EDTA. With minor exceptions, there is a good correspondence between the combined peaks of the two complementary fragment spectra and the spectrum of the intact 5S RNA (e.g., peaks A, B, and C), confirming that the fragments retain their secondary structures even after cleavage from the rest of the molecule.

positions are highly sensitive to the type (A·U, G·C, or G·U) and sequence of base pairs, we conclude that the spatial arrangement of the polyribonucleotide chains in the core and common-arm fragments must be essentially the same as in the intact 5S RNA molecule.

The most obvious conclusion to be drawn from the above observation is that a common-arm base-paired segment indeed exists; thus, any 5S RNA secondary structural models which do not contain such a segment can be ruled out. Second, it is clear that wheat germ 5S RNA possesses at least two independently stable structural domains, in accord with recent differential scanning calorimetric experiments (Li & Marshall, 1985). Finally, it appears unlikely that the common-arm and core domains are strongly connected by tertiary base pairing, because the two fragments are easily separated under nondenaturing conditions. However, peaks "M", "N", and "T" in the intact 5S RNA are not seen in either of the two complementary fragments and may be tertiary base pairs.

Structure of Core and Common-Arm Fragments Is the Same As in Intact 5S RNA. Before proceeding to analyze the structure of the two RNA fragments, we need to establish that the fragments still retain the same structure as in the intact 5S RNA. Although the previously discussed complementarity of the fragment NMR spectra (Figure 3) supports this idea, the best evidence is furnished by homonuclear Overhauser enhancement (NOE) experiments. Since NOE effects propagate via dipole–dipole interactions (Noggle & Schirmer, 1971; Bothner-By, 1979), the NOE difference spectrum will be extremely sensitive to any change in identity (A·U, G·C, or G·U) of base pairs via intrabase NOE signals and to any change in base pair sequence via interbase NOE's (Johnston & Redfield, 1978, 1981). Figure 4 shows the NOE difference spectra resulting from irradiation of peak "A" of intact wheat germ 5S RNA (top) or the common-arm fragment (bottom). Peak A can be identified as an A·U base pair proton, based on the sharp NOE difference peak at 7.3 ppm from the aromatic C-2 adenine proton. Weaker (but identical) interbase NOE connectivity from peak A to peaks "K" and "L" is observed for both the common-arm and intact 5S RNA.

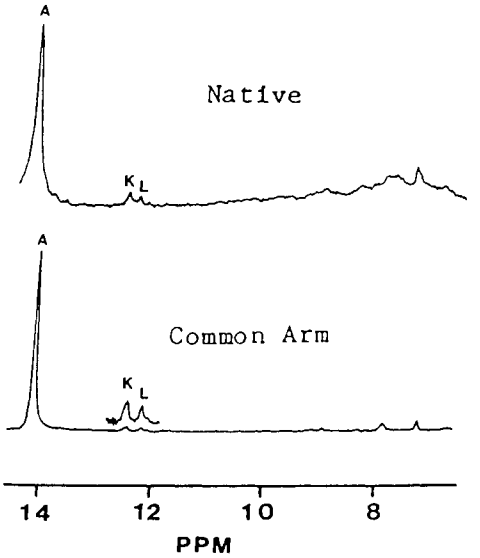

FIGURE 4: 500-MHz ^{1}H homonuclear NOE difference spectra obtained via on- and off-resonance irradiation of peak A of intact wheat germ 5S RNA (top) and its common-arm fragment (bottom). The similarity between the two NOE patterns shows that the spatial arrangement of the common-arm RNA fragment is retained after cleavage from the rest of the molecule.

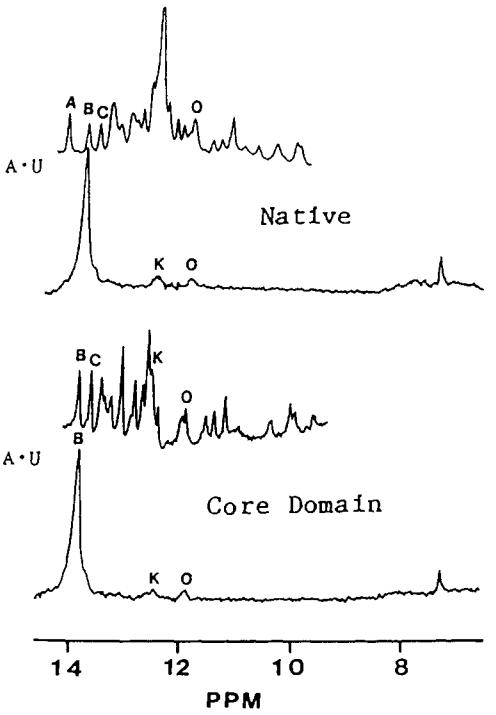

FIGURE 5: 500-MHz ^{1}H homonuclear NOE difference spectra obtained via on- and off-resonance irradiation of peak B of intact wheat germ 5S RNA (top) and its core fragment (bottom). The similarity between the two NOE patterns demonstrates that the core fragment retains its spatial configuration after cleavage from the rest of the molecule.

Thus, the same A·U resonance(s) is (are) found in the common-arm fragment as in intact 5S RNA, and their nearest-neighbor base pairs are also conserved. On the basis of the NOE results, the common arm must retain its native structure even after cleavage from the rest of the 5S RNA molecule.

Homologous NOE experiments for the core fragment are shown in Figure 5. The sharp NOE difference signal at ca. 7.4 ppm identifies "B" as an A·U base pair proton both in the core fragment and in the intact 5S RNA. The identical interpair NOE connectivity from B to peaks K and O in both

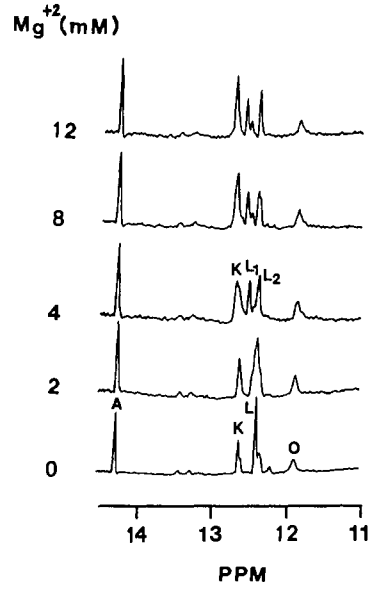

FIGURE 6: Evolution of the 500-MHz proton NMR spectrum of the common-arm fragment of wheat germ 5S RNA upon titration with Mg^{2+}. Mg^{2+} was eliminated from the 5S RNA in the lower-most spectrum. $MgCl_2$ was added to the remaining samples at concentrations of 2, 4, 8, and 12 mM. As $MgCl_2$ concentration is varied, peaks K and L split into several component peaks—direct evidence that the common-arm fragment contains more than four base pairs.

spectra confirms that the nearest-neighbor base pairs are the same in the "core" fragment as in the intact 5S RNA. Peak C and its NOE-connected partners are also conserved between the core fragment and the intact 5S RNA. Thus, at least the segments containing base pairs B and C of the core fragment must have the same structure as in the intact 5S RNA. Finally, the detection of peak C in the core fragment confirms its previous assignment in the $C_{18}G_{60}$-$A_{19}U_{59}$-$C_{20}G_{58}$ sequence of the tuned helix segment (Li & Marshall, 1986).

Structure of the Common-Arm Fragment: Number of Base Pair Hydrogen-Bond Protons. At first glance, the few peaks seen in the 500-MHz ^1H NMR spectrum of the common-arm fragment (Figure 3, bottom) might appear to match the most commonly proposed model which has one A·U and three G·C pairs. However, closer inspection suggests that the spectrum could arise from superposition of several peaks with very similar chemical shifts. In order to separate these putatively overlapping resonances, we therfore induced selective shifts via addition of Mg^{2+} and variation in temperature.

Figure 6 shows the ^1H NMR spectra resulting from Mg^{2+} titration of the common-arm fragment. Peak K is partially resolved into two resonances when Mg^{2+} is removed from the sample, and the peak broadens and shifts on addition of Mg^{2+}. Peak "L" clearly separates into at least two peaks ("L_1" and "L_2") on addition of Mg^{2+}. On the basis of a relative intensity of 1 for (e.g.) peak L_1, peak A appears to consist of two overlapped A·U base pair proton resonances. Thus, six to seven hydrogen-bonded imino protons appear to be present in the common-arm fragment—certainly more than the 4 base pairs of the minimal Fox–Woese model (see below).

Figure 7 shows the effect of increasing temperature on the ^1H NMR spectrum of the common-arm fragment. Its melting behavior is strikingly similar to that seen for the intact 5S RNA molecule (Li & Marshall, 1986). Peak A melts at ca. 49 °C, whereas peaks K and L persist even at 60 °C, in accord with our identification of A as A·U's and K and L as G·C base pair protons based on their chemical shifts and intrapair NOE's (see below). It is important to recognize that base pairs from the *same* helical segment are seen to melt at widely *different*

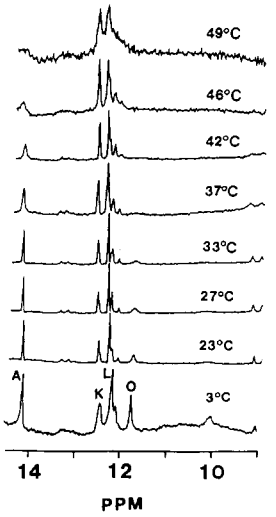

FIGURE 7: Temperature dependence of the 500-MHz proton NMR spectrum of wheat germ 5S RNA. Temperature-induced melting establishes that peaks K and L (assigned as G·C pairs) are more stable than the two resonances at peak A (assigned as A·U pairs) and that peak O melts at low temperature.

Table I: Experimental and Ring Current Calculated Base Pair Hydrogen-Bond Proton Chemical Shifts for the Common Arm of Wheat Germ Ribosomal 5S RNA, Based on the Secondary Structural Models of Figure 8

base pair	chemical shift computed from ring currents[a] (ppm)	exptl chemical shift[b] (ppm)
C_{29}·G_{48}	12.52	12.35 (peak L)
G_{30}·C_{47}	12.51	12.53 (peak K)
G_{31}·C_{46}	12.36	12.35 (peak L)
A_{32}·U_{45}	14.14	14.21 (peak A)
A_{42}·U_{33}	14.16	14.21 (peak A)
G_{41}·C_{34}	12.58	12.53 (peak K)

[a] Computed according to Arter and Schmidt (1976), assuming intrinsic A·U and G·C positions of 14.35 and 13.45 ppm, respectively (Reid et al., 1979). [b] See Figure 3.

temperatures. Therefore, previous attempts to assign an individual optical melting or differential scanning calorimetry transition to the melting of a particular RNA base-paired helical segment of an RNA [e.g., see Privalov & Filimonov (1978)] are clearly suspect. Finally, peak O is unstable at all but the lowest temperature and may arise from an unpaired base (U_{38}; see below) in the hairpin loop (Haasnoot et al., 1980).

Assignment of Common-Arm Resonances to Specific Base Pairs. At this stage, ring current calculations (Arter & Schmidt, 1976) serve to confirm and extend the identification and assignment of the common-arm resonances. Table I compares the observed chemical shifts to those computed for the base-pairing model shown in Figure 8 (bottom). For the ring current calculations, we assume that the RNA helix extending from C_{29}·G_{48} to G_{41}·C_{34} is continuous, i.e., that the two-base bulge at $A_{43}C_{44}$ does not affect the stacking of the other (paired) bases.

Although most of the common-arm resonances can be assigned via ring current predictions (Table I), there is an immediate discrepancy between the experimental NOE results and the minimal common-arm model shown at the top of Figure 8. Irradiation of the A·U resonance at A (Figure 4) produces primary interbase NOE's to *two* G·C resonances, K and L. However, if peak A represents A_{32}·U_{45}, then it has only *one* nearest-neighbor G·C at G_{31}·C_{46}. Therefore, peak A must represent *two* overlapped resonances, as was previously inferred from relative peak heights. An alternative explanation is spin

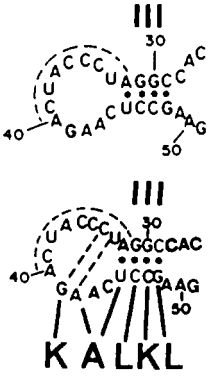

FIGURE 8: Fox and Woese model (top) and presently proposed model (bottom) for the secondary structure of the common-arm portion of wheat germ 5S RNA. The new structure contains two more base pairs than the original Fox and Woese model. Assigned proton NMR resonances are labeled as in Figure 3.

diffusion, in which the NOE effect propagates to second-nearest neighbors. However, spin diffusion appears unlikely, because (a) G_{30}·C_{47} is too far away to produce the relatively large interbase NOE seen in Figure 4, and (b) NOE experiments at lower decoupler power and shorter irradiation time of peak A gave qualitatively similar results. Another possibility is that K or L arise, from hairpin loop imino protons which are not fully exchangeable with water (Haasnoot et al., 1980). The only three bases with available imino protons are U_{33}, U_{38}, and G_{41}. We offer two results suggesting that G_{41} in wheat germ 5S RNA may be intramolecularly base paired. First, G_{41} is not attacked by RNase T1, even under the (present) conditions which produced the core and common-arm fragments in high yield. Second, we find that the Watson–Crick-complementary pentamer poly(rU_5) does *not* bind to A_{40}GAA to produce additional A·U and/or G·U resonances in the common-arm spectrum (not shown), in contrast to the base pairs formed by mixing two tRNAs whose anticodons are Watson–Crick complementary (Schimmel & Redfield, 1980; Schwarz & Gassen, 1977). Another possible source of the extra resonances in the common-arm spectrum might be the presence of multiple conformers [but not the dynamic situation proposed by Vandenberghe et al. (1984), which would require longer fragment length], but it seems unlikely that such multiple conformers would be the same in the common-arm fragment as in the intact 5S RNA. Finally, the common-arm spectrum at 1:8 dilution (not shown) was the same as shown in Figure 4; moreover, no dimer band was seen on nondenaturing PAGE. Thus, the additional resonances do not arise from dimers or polymers of the common-arm fragment.

We can accommodate all of the above results by adding to the common-arm hairpin loop two base pairs (G_{41}·C_{34} and A_{42}·U_{33}), whose ring current calculated chemical shifts are 12.58 and 14.16 ppm, respectively. For this model, the A_{32}·U_{45} resonance overlaps with the A_{42}·U_{33} resonance to form peak A (see Table I). Thus, irradiation of peak A should result in NOE signals from peaks K and L, as observed experimentally in Figure 4. The superposition of two peaks at A also accounts for the relatively broad adenine C-2 NOE peak in Figure 4 (compare to the narrower adenine C-2 NOE from the single A·U resonance in Figure 5), since it consists of two overlapped signals. On the basis of its chemical shift, the remaining peak O (which is very temperature labile) could arise from a U_{38} or G_{51} imino proton. However, since G_{51} is a terminal residue and therefore likely to undergo rapid imino proton exchange with H_2O, it is logical to assign peak O to U_{38}.

Figure 8 shows the original (top) and new (bottom) base-pairing scheme for the common-arm segment of wheat germ 5S RNA. The addition of two base pairs, $G_{41}C_{34}$-$A_{42}U_{33}$, to the original Fox and Woese model accounts for all of the present proton NMR results. Moreover, addition of the two base pairs $G_{41}C_{34}$-$A_{42}U_{33}$ reduces the hairpin loop size from 12 bases down to 6, the most stable number for a hairpin loop (Haasnoot et al., 1985). Comparative sequence analysis reveals that the newly proposed base pairs are conserved for eukaryotes (Delihas & Andersen, 1982; Erdmann et al., 1985), suggesting that the secondary structure of Figure 8 (bottom) could be universal, at least for eukaryotic 5S RNA.

Implications of the Present Results. Proposed additional base pairs in the loop extending from the 5S RNA common arm (de Wachter et al., 1982) were originally inferred from comparison of evolutionarily conserved 5S RNA primary base sequences. The present direct observation and assignment of two additional common-arm base pairs (via proton NMR of native and common-arm fragments, spectral Mg^{2+} and temperature dependence, and homonuclear Overhauser enhancements) strongly support this model. Intraloop base pairing nicely accounts for the observation that 5S RNA G_{41}AAC interaction with tRNA GTΨC is not necessary for protein synthesis (Zagorska et al., 1984; Pace et al., 1982), since G_{41} and A_{42} are now seen to be needed for internal hydrogen bonding in 5S RNA. Furthermore, since 5S RNAs from several higher plants have a G_{41}AAC segment instead of the G_{41}AUC generally found in eukaryotic 5S RNAs, eukaryotic initiator tRNA (whose structure contains GAΨC rather than GTΨC) is not even complementary to the GAAC of plant 5S RNA, and one would not expect to find binding between the two segments (Noller, 1984).

ACKNOWLEDGMENTS

We thank E. S. Maxwell for his generous assistance in training one of us (J.W.) to perform RNA sequencing of the common-arm fragment in his laboratory. We also thank C. E. Cottrell, L.-H. Chang, and S.-M. Chen for valuable discussions and assistance, and we thank International Multifoods, Columbus, OH, for their generous donation of wheat germ.

Registry No. Adenine, 73-24-5; guanine, 73-40-5; cytosine, 71-30-7; uracil, 66-22-8.

REFERENCES

Arter, D. B., & Schmidt, P. G. (1976) *Nucleic Acids Res. 3*, 1437–1447.

Barber, C., & Nichols, J. L. (1978) *Can. J. Biochem. 56*, 357–364.

Boedtker, H., & Kelling, D. G. (1967) *Biochem. Biophys. Res. Commun. 29*, 758–766.

Bothner-By, A. A. (1979) in *Biological Applications of Magnetic Resonance* (Shulman, R. G., Ed.) pp 177–219, Academic Press, New York.

Brownlee, G. G., Sanger, F., & Barrell, B. G. (1968) *J. Mol. Biol. 34*, 379–412.

Brownlee, G. G., Cartwright, E., McShane, T., & Williamson, R. (1972) *FEBS Lett. 25*, 8–12.

Buy, B., & Weissman, S. M. (1971) *J. Biol. Chem. 246*, 747.

Chang, L.-H., & Marshall, A. G. (1986) *Biochemistry 25*, 3056–3063.

Chen, S.-M., & Marshall, A. G. (1986) *Biochemistry 25*, 5117–5125.

Delihas, N., & Andersen, J. (1982) *Nucleic Acids Res. 10*, 7323–7344.

Delihas, N., Andersen, J., & Singhal, R. P. (1984) *Prog. Nucleic Acid Res. Mol. Biol. 31*, 161–190.

De Wachter, R., Chen, M.-W., & Vandenberghe, A. (1982) *Biochimie 64*, 311–329.

du Buy, B., & Weissman, S. M. (1971) *J. Biol. Chem. 246*, 747–761.
Erdmann, V. A., Sprinzl, M., & Pongs, O. (1973) *Biochem. Biophys. Res. Commun. 54*, 942–948.
Erdmann, V. A., Wolters, J., Huysmans, E., & De Wachter, R. (1985) *Nucleic Acids Res. 13*, r105–r153.
Fox, G. E., & Woese, C. R. (1975) *Nature (London) 256*, 505–507.
Haasnoot, C. A. G., Den Hartoy, J. H. J., De Rooy, F. M., Van Boom, J. H., & Altona, C. (1980) *Nucleic Acids Res. 8*, 169–181.
Haasnoot, C. A. G., Van der Marel, G. A., Van Boom, J. H., & Hilbers, C. W. (1985) in *Fourth Conversation in Biomolecular Stereodynamics* (Sarma, R. H., Ed.) p 121, Adenine Press, New York.
Hore, P. J. (1983) *J. Magn. Reson. 54*, 539–542.
Johnston, P. D., & Redfield, A. G. (1978) *Nucleic Acids Res. 5*, 3913–3927.
Johnston, P. D., & Redfield, A. G. (1981) *Biochemistry 20*, 1147–1156.
Lee, K. M., & Marshall, A. G. (1986) *Biochemistry 25*, 8245–8252.
Lee, K. M., & Marshall, A. G. (1987) *Biochemistry* (in press).
Li, S.-J., & Marshall, A. G. (1985) *Biochemistry 24*, 4047–4052.
Li, S.-J., & Marshall, A. G. (1986) *Biochemistry 25*, 3673–3682.
Li, S.-J., Chang, L.-H., Chen, S.-M., & Marshall, A. G. (1984) *Anal. Biochem. 138*, 465–471.
Luehrsen, K. R., & Fox, G. E. (1981) *Proc. Natl. Acad. Sci. U.S.A. 78*, 2150–2154.
Luoma, G. A., & Marshall, A. G. (1978a) *Proc. Natl. Acad. Sci. U.S.A. 75*, 4901–4905.
Luoma, G. A., & Marshall, A. G. (1978b) *J. Mol. Biol. 125*, 95–105.
Mackay, R. M., Spencer, D. F., Doolittle, W. F., & Gray, M. W. (1980) *Eur. J. Biochem. 112*, 561–576.
Mackay, R. M., Spencer, D. F., Schnare, N. N., Doolittle, W. F., & Gray, M. W. (1982) *Can. J. Biochem. 60*, 480–489.
Monier, R. (1974) in *Ribosomes* (Nomura, M., Lengyel, P., & Tissieres, A., Eds.) p 141, Cold Spring Harbor Press, Cold Spring Harbor, NY.
Noggle, J. H., & Schirmer, R. E. (1971) *The Nuclear Overhauser Effect: Chemical Applications*, Academic Press, New York.
Noller, H. F. (1984) *Annu. Rev. Biochem. 53*, 119–162.
Ofengand, J., & Henes, C. (1969) *J. Biol. Chem. 244*, 6241–6253.
Osterberg, R., Sjoberg, B., & Garrett, R. A. (1976) *Eur. J. Biochem. 68*, 481–487.
Pace, B., Matthews, E. A., Johnson, K. D., Cantor, C. R., & Pace, N. R. (1982) *Proc. Natl. Acad. Sci. U.S.A. 79*, 36–40.
Payne, P. I., & Dyer, T. A. (1976) *Eur. J. Biochem. 71*, 33–38.
Pieler, T., & Erdmann, V. A. (1982) *Proc. Natl. Acad. Sci. U.S.A. 79*, 4599–4603.
Pieler, T., Digweed, M., & Erdmann, V. A. (1984) in *Gene Expression* (Clark, B. F. C., & Petersen, H. U., Eds.) pp 353–376, Munksgaard, Copenhagen.
Privalov, P. L., & Filimonov, V. V. (1978) *J. Mol. Biol. 122*, 447–464.
Redfield, A. G., Kunz, S. D., & Ralph, E. K. (1975) *J. Magn. Reson. 19*, 114–117.
Reid, B. R., McCollum, L., Ribeiro, N. S., Abbate, J., & Hurd, R. E. (1979) *Biochemistry 18*, 3996–4005.
Roth, K., Kimber, B. J., & Feeney, J. (1980) *J. Magn. Reson. 41*, 302–309.
Schimmel, P. R., & Redfield, A. G. (1980) *Annu. Rev. Biophys. Bioeng. 9*, 181–221.
Schwarz, U., & Gassen, H. G. (1977) *FEBS Lett. 78*, 267–270.
Studnicka, G. M., Eiserling, F. A., & Lake, J. A. (1981) *Nucleic Acids Res. 9*, 1885–1904.
Vandenberghe, A., Chen, M.-W., Dams, E., De Baere, R., De Roeck, E., Huysmans, E., & De Wachter, R. (1984) *FEBS Lett. 171*, 17–23.
Zagorska, L., Duin, J. V., Noller, H. F., Pace, B., Johnson, K. D., & Pace, N. R. (1984) *J. Biol. Chem. 259*, 2798–2802.